An Efficient Volume Integral Equation Technique for the Analysis of Tapered Dielectric Rod Antennas

Alireza Bostani
Department of Electrical and Computer Engineering
Isfahan University of Technology
Isfahan, Iran 84156-83111
a.bostani@ec.iut.ac.ir

Amir Borji
Department of Electrical and Computer Engineering
Isfahan University of Technology
Isfahan, Iran 84156-83111
aborji@cc.iut.ac.ir

***Abstract* — A computationally efficient method for the analysis of tapered dielectric rod antennas is presented. The method combines the so-called local mode theory with the method of moments. Radiation patterns for dielectric rod antennas of varying radius and different taper profiles are presented. The method is validated by comparison with the data obtained from a surface integral equation technique. Moreover, it is demonstrated that the method is applicable for different types of excitations.**

Keywords—Antenna theory, dielectric rod antennas, end-fire antennas, local mode theory, method of moments

I. INTRODUCTION

TAPERED dielectric antennas have been known for many years, but a good antenna theory has not been available for their analysis because a convenient representation in a separable geometry is not possible for the tapered rod. However, with the availability of solid state energy sources and the development of low-loss silicon, interest in tapered dielectric antennas has increased. This is mainly due to their simple configuration, ease of manufacture, compact size, and high gain. Furthermore, they can be easily integrated with dielectric waveguides used in millimeter wave devices [1]–[3].

In tapered dielectric antennas, the cross-section of the waveguide in forward direction is gradually decreased. For a feed that is a uniform dielectric waveguide of the same material which is connected to the bottom of the antenna, the tapered region smoothly transforms the guided, strongly bound surface wave into a free space propagating wave with negligible reflection. This antenna produces a relatively broad end-fire radiation pattern with low side lobe levels [1].

Although numerous experimental studies on tapered rod antennas have been presented, available theoretical studies usually include many simplifications and only give us some general guidelines for design [1],[5],[6]. Dielectric rod antennas are usually designed based on the concept of radiation from discontinuities [4]. In this approach the antenna is considered as a linear array of effective sources which are the feed radiation due to power not converted into the surface wave by the exciting feed and the radiation from infinitesimal discontinuities experienced by the surface wave travelling along the antenna.

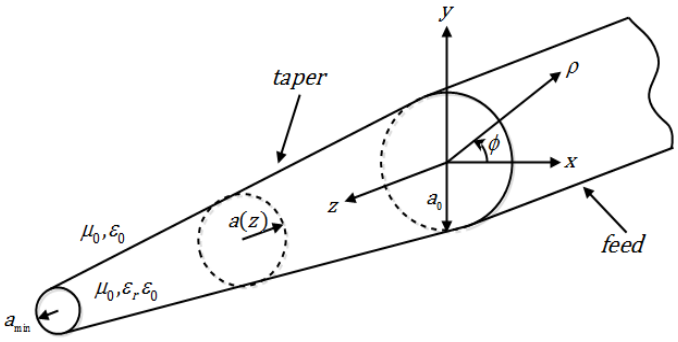

Fig. 1: Tapered dielectric rod antenna fed by a uniform circular waveguide.

A number of rigorous numerical methods such as FDTD [7]-[9], integral equation based methods [10,11], and FEM [12] have also been employed to study the radiation properties of dielectric rod antennas. Although these methods are accurate, they are computationally intensive and present little further insight about fundamental working mechanisms. Consequently, less rigorous but still accurate alternative analytical methods using local mode theory have been proposed to analyze the tapered dielectric wedge [13] and tapered rod antenna [14]. However, the result in [13] is only in two-dimension and the analysis in [14] is very brief with no details.

In this paper, a simplified semi-rigorous approach to the analysis of tapered dielectric antennas is proposed and applied to the dielectric rod configuration of Fig. 1. In this approach a simple volume integral equation with point matching solution is used to analyze the tapered dielectric rod antenna. The method uses a local mode theory to determine the appropriate basis function for the polarization current distribution in the dielectric region and, after applying the method of moments, utilizes the equivalence principle to calculate the far-field radiation pattern from this current distribution [15], [16]. The method results in a formula for the radiation pattern that needs only simple integrations over the cross section of the antenna. The proposed method is easy to implement but shows good accuracy as the numerical results are compared with those obtained from a commercial EM simulator.

In Section II, the problem geometry and excitation are described and the integral equation approach is presented, resulting in expressions for the radiation pattern. These formulas are used to compute the patterns that are presented in

978-1-4673-2073-3/12/$31.00 ©2012 IEEE

Section III. For validation, normalized radiation patterns obtained from CST Microwave Studio are also presented.

II. THEORY

Generally, when the physical properties of a dielectric waveguide change in the direction of propagation, the pure guided modes of a uniform waveguide no longer exist. However, with the slowly varying transverse properties in the tapered rod, the so-called *local mode theory* is a good approximation for the solution of the propagating wave along the taper [13, 14]. Basically, the local mode theory for a tapered waveguide is based on the following assumptions: (a) the fields over a local transverse plane of the rod behave as the guided mode in a uniform infinite waveguide with the same cross section; (b) the radiation loss along the taper is negligible [14].

In this analysis, the radius a_0 at the input of the tapered rod will be chosen to support only the fundamental HE_{11} mode above cutoff at the operating frequency. As a result, under the local mode approximation, fields in a transverse plane of the tapered waveguide are similar to those in uniform section but they are updated with the local radius a(z). The HE_{11} mode is degenerate (e.g. HE_{11}^{x} and HE_{11}^{y}) due to the circular symmetry [17]. For HE_{11}^{y} mode whose dominant field components are E_y and H_x , the field expressions are [17]:

For $\rho \le a$ (core region):

$$\begin{aligned}
E_x(\rho,\varphi) &= -jE_0\frac{\beta}{2k_\rho}(1+s)J_2(k_\rho\rho)sin\,(2\varphi)\\
E_y(\rho,\varphi) &= jE_0\frac{\beta}{2k_\rho}\big[(1-s)J_0(k_\rho\rho)\\
&\qquad +(1+s)J_2(k_\rho\rho)cos\,(2\varphi)\big]\\
E_z(\rho,\varphi) &= -E_0J_1(k_\rho\rho)sin\,(\varphi)\\
H_x(\rho,\varphi) &= -jE_0\frac{\omega\varepsilon_0\varepsilon_r}{2k_\rho}\big[(1-s_1)J_0(k_\rho\rho)\\
&\qquad +(1+s_1)J_2(k_\rho\rho)cos\,(2\varphi)\big]\\
H_y(\rho,\varphi) &= -jE_0\frac{\omega\varepsilon_0\varepsilon_r}{2k_\rho}(1+s_1)J_2(k_\rho\rho)sin\,(2\varphi)\\
H_z(\rho,\varphi) &= -E_0\frac{\beta s}{\omega\mu_0}J_1(k_\rho\rho)cos\,(\varphi)
\end{aligned} \tag{1}$$

For $\rho > a$ (cladding region):

$$\begin{aligned}
E_x(\rho,\varphi) &= jE_0\frac{\beta}{2\alpha_\rho}\frac{J_1(k_\rho a)}{K_1(\alpha_\rho a)}(1+s)K_2(\alpha_\rho\rho)sin\,(2\varphi)\\
E_y(\rho,\varphi) &= jE_0\frac{\beta}{2\alpha_\rho}\frac{J_1(k_\rho a)}{K_1(\alpha_\rho a)}\big[(1-s)K_0(\alpha_\rho\rho)\\
&\qquad -(1+s)K_2(\alpha_\rho\rho)cos\,(2\varphi)\big]\\
E_z(\rho,\varphi) &= -E_0\frac{J_1(k_\rho a)}{K_1(\alpha_\rho a)}K_1(\alpha_\rho\rho)sin\,(\varphi)\\
H_x(\rho,\varphi) &= -jE_0\frac{\omega\varepsilon_0}{2\alpha_\rho}\frac{J_1(k_\rho a)}{K_1(\alpha_\rho a)}\big[(1-s_0)K_0(\alpha_\rho\rho)\\
&\qquad -(1+s_0)K_2(\alpha_\rho\rho)cos\,(2\varphi)\big]\\
H_y(\rho,\varphi) &= jE_0\frac{\omega\varepsilon_0}{2\alpha_\rho}\frac{J_1(k_\rho a)}{K_1(\alpha_\rho a)}(1+s_0)K_2(\alpha_\rho\rho)sin\,(2\varphi)\\
H_z(\rho,\varphi) &= -E_0\frac{\beta s}{\omega\mu_0}\frac{J_1(k_\rho a)}{K_1(\alpha_\rho a)}K_1(\alpha_\rho\rho)cos\,(\varphi)
\end{aligned} \tag{2}$$

Where s, s_0 and s_1 are:

$$\begin{aligned}
s &= \left(\frac{1}{u^2}+\frac{1}{v^2}\right)\left[\frac{J_1'(u)}{uJ_1(u)}+\frac{K_1'(v)}{vK_1(v)}\right]^{-1}\\
s_0 &= \frac{\beta^2}{k_0^2}s\\
s_1 &= \frac{\beta^2}{\varepsilon_r k_0^2}s
\end{aligned} \tag{3}$$

In which $u = k_\rho a$ and $v = \alpha_\rho a$. The propagation constant β is determined by the dispersion relation [17]:

$$\left[\frac{\varepsilon_r J_1'(u)}{uJ_1(u)}+\frac{K_1'(v)}{vK_1(v)}\right]\left[\frac{J_1'(u)}{uJ_1(u)}+\frac{K_1'(v)}{vK_1(v)}\right] = \left(\frac{\varepsilon_r}{u^2}+\frac{1}{v^2}\right)\left(\frac{1}{u^2}+\frac{1}{v^2}\right)$$

While the lateral wave numbers are given by:

$$k_\rho^2 = \varepsilon_r k_0^2 - \beta^2$$

$$\alpha_\rho^2 = \beta^2 - k_0^2$$

The quantities $\beta(z)$, $k_\rho(z)$ and $\alpha_\rho(z)$ are also determined by the above equations. Note that with the local rod radius now dependent on "z", the propagation constant $\beta(z)$ also becomes a function of z in the tapered region and so do the lateral wavenumbers $k_\rho(z)$ and $\alpha_\rho(z)$.

A. Volume Integral Equation Formulation

Placing a dielectric object in front of a radiating open-ended waveguide modifies its radiation pattern. This suggests that the radiation from a dielectric rod antenna can also be treated as a scattering problem. As shown in Fig. 2, the tapered dielectric rod section is illuminated by the incident wave $\vec{E}^i$ generated by the equivalent surface currents over the feeding aperture at $z = 0$. The material inhomogeneity formed by the dielectric rod scatters the incident field and produces the scattered wave denoted by $\vec{E}^s$. The total radiation field is the superposition of the two components. In the case of scattering from a dielectric object, the equivalent volume current density responsible for the scattered fields is given by [18]:

$$\vec{J}_{eq} = j\omega\varepsilon_0(\varepsilon_r - 1)\vec{E}^t = j\omega\varepsilon_0(\varepsilon_r - 1)(\vec{E}^i + \vec{E}^s) \tag{4}$$

Where ε_r is the relative dielectric constant and ε_0 is the permittivity of free space. The electric field due to the equivalent current is given by:

$$\vec{E}^s = -j\omega\left(\vec{A}^s + \frac{1}{k_0^2}\nabla\nabla.\vec{A}^s\right) \tag{5}$$

$$\vec{A}^s = \frac{\mu_0}{4\pi}\iiint \vec{J}_{eq}(\acute{r})\frac{e^{-jk_0|r-\acute{r}|}}{|r-\acute{r}|}d\acute{v} \tag{6}$$

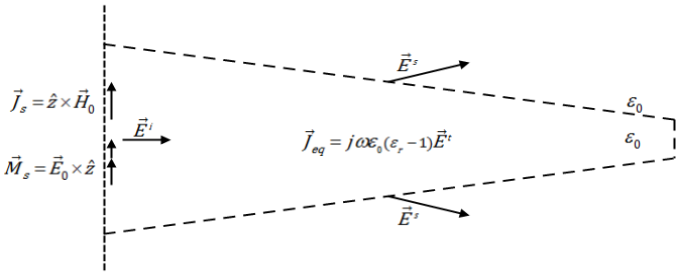

Fig. 2: Volume and surface current equivalence for tapered rod antenna.

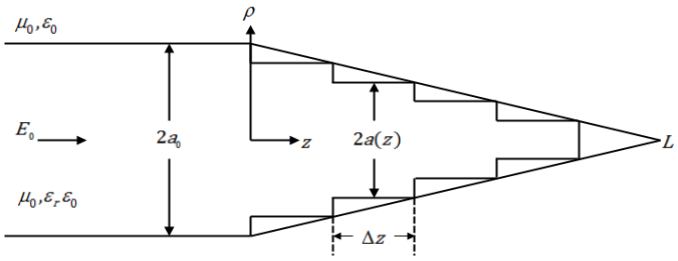

Fig. 3: Staircase model of the tapered dielectric rod antenna.

Hence an integral equation for $\vec{J}_{eq}$ is [18]:

$$-\vec{E}^s + \frac{\vec{J}_{eq}}{j\omega\varepsilon_0(\varepsilon_r - 1)} = \vec{E}^i \tag{7}$$

B. Method of Moments Solution

Solution of the scattering problem is accomplished by modeling the tapered region with the staircase approximation shown in Fig. 3 and using the Point-Matching method. Each section, which is a basis function, is modeled as a planar radiating disk with local radius $a(z)$ and thickness dz . As mentioned before, it is assumed that the local mode approximation gives a good estimation of the total field $\vec{E}^t$ in the core region. As a result, a simple semi-analytical formulation is obtained without resorting to a complex numerical solution for the integral equation.

According to (4), for each disk $\vec{J}_{eq}$ is approximated by the total electric field expressions in the core region given in (1) but with an unknown complex coefficient $A(z)$. This unknown coefficient will be computed by applying the point-matching technique at the center of each disk. Assuming that $E_0 = 1$, the expressions for Cartesian components of $\vec{J}_{eq}$ are:

$$\begin{aligned} J_x(\rho,\varphi) &= -jA(z)\frac{\beta}{2k_\rho}(1+s)J_2(k_\rho\rho)sin\,(2\varphi) \\ J_y(\rho,\varphi) &= jA(z)\frac{\beta}{2k_\rho}\left[(1-s)J_0(k_\rho\rho)\right. \\ &\quad \left. + (1+s)J_2(k_\rho\rho)cos\,(2\varphi)\right] \\ J_z(\rho,\varphi) &= -A(z)J_1(k_\rho\rho)sin\,(\varphi) \end{aligned} \tag{8}$$

To apply the point-matching technique we enforce (7) at the center of each disk and, because of using the local mode theory, this is only done for one of the components of the electric field. Here we have applied the point-matching method for E_y . Thus, for each disk we have one equation with only one unknown $A(z)$. This is basically a one dimensional moment method that is much simpler and computationally more efficient compared to a three dimensional one. Choosing the center of each disk for point-matching is arbitrary and we have only used it because of simplicity and efficient calculation of the integrals as a result of the symmetry around the z-axis.

The equivalent surface currents $\vec{J}_s$ and $\vec{M}_s$ on the transverse plane $z = 0$ which generate $\vec{E}^i$, are given by [17]:

For $\rho \le a$ (core region):

$$\begin{aligned} J_x(\rho,\varphi) &= j\frac{\omega\varepsilon_0\varepsilon_r}{2k_\rho}(1+s_1)J_2(k_\rho\rho)sin\,(2\varphi) \\ J_y(\rho,\varphi) &= -j\frac{\omega\varepsilon_0\varepsilon_r}{2k_\rho}\left[(1-s_1)J_0(k_\rho\rho)\right. \\ &\quad \left. + (1+s_1)J_2(k_\rho\rho)cos\,(2\varphi)\right] \\ M_x(\rho,\varphi) &= j\frac{\beta}{2k_\rho}\left[(1-s)J_0(k_\rho\rho)\right. \\ &\quad \left. + (1+s)J_2(k_\rho\rho)cos\,(2\varphi)\right] \\ M_y(\rho,\varphi) &= j\frac{\beta}{2k_\rho}(1+s)J_2(k_\rho\rho)sin\,(2\varphi) \end{aligned} \tag{9}$$

For $\rho > a$ (cladding region):

$$\begin{aligned} J_x(\rho,\varphi) &= -j\frac{\omega\varepsilon_0}{2\alpha_\rho}\frac{J_1(k_\rho a)}{K_1(\alpha_\rho a)}(1+s_0)K_2(\alpha_\rho\rho)sin\,(2\varphi) \\ J_y(\rho,\varphi) &= -j\frac{\omega\varepsilon_0}{2\alpha_\rho}\frac{J_1(k_\rho a)}{K_1(\alpha_\rho a)}\left[(1-s_0)K_0(\alpha_\rho\rho)\right. \\ &\quad \left. - (1+s_0)K_2(\alpha_\rho\rho)cos\,(2\varphi)\right] \\ M_x(\rho,\varphi) &= j\frac{\beta}{2\alpha_\rho}\frac{J_1(k_\rho a)}{K_1(\alpha_\rho a)}\left[(1-s)K_0(\alpha_\rho\rho)\right. \\ &\quad \left. - (1+s)K_2(\alpha_\rho\rho)cos\,(2\varphi)\right] \\ M_y(\rho,\varphi) &= -j\frac{\beta}{2\alpha_\rho}\frac{J_1(k_\rho a)}{K_1(\alpha_\rho a)}(1+s)K_2(\alpha_\rho\rho)sin\,(2\varphi) \end{aligned} \tag{10}$$

The proposed method is valid for any kind of feed that excites the HE_{11} mode efficiently such as dipole excitation or circular metallic waveguide aperture. Here it is assumed that the rod is excited with 100% excitation efficiency and only the dominant mode is propagating along the rod, *i.e.* the excitation is assumed to be ideal and the results will be a little different with the actual feeding mechanism in place.

C. Radiation Pattern Calculation

After finding $A(z)$ the far field radiation pattern can be calculated from the feed radiation fields plus the radiation fields due to the tapered structure. Because of the modal behavior assumed for $\vec{J}_{eq}$, a closed form expression for the far field pattern is derived that can be evaluated analytically. For the feeding circular waveguide we have:

$$N_x^i = -j\pi\omega\varepsilon_0\left[\frac{\varepsilon_r(1+s_1)I_3}{k_\rho} - \frac{J_1(k_\rho a)(1+s_0)I_4}{\alpha_\rho K_1(\alpha_\rho a)}\right]sin\,(2\varphi)$$

$$N_y^i = -j\pi\omega\varepsilon_0\left[\frac{\varepsilon_r(1-s_1)I_1}{k_\rho} + \frac{J_1(k_\rho a)(1-s_0)I_2}{\alpha_\rho K_1(\alpha_\rho a)} - \left(\frac{\varepsilon_r(1+s_1)I_3}{k_\rho} - \frac{J_1(k_\rho a)(1+s_0)I_4}{\alpha_\rho K_1(\alpha_\rho a)}\right)cos(2\varphi)\right] \quad (11)$$

$$L_x^i = j\pi\beta\left[(1-s)\left(\frac{I_1}{k_\rho} - \frac{J_1(k_\rho a)I_2}{\alpha_\rho K_1(\alpha_\rho a)}\right) - (1+s)\left(\frac{I_3}{k_\rho} - \frac{J_1(k_\rho a)I_4}{\alpha_\rho K_1(\alpha_\rho a)}\right)cos\,(2\varphi)\right]$$

$$L_y^i = -j\pi\beta(1+s)\left[\frac{I_3}{k_\rho} - \frac{J_1(k_\rho a)I_4}{\alpha_\rho K_1(\alpha_\rho a)}\right]sin\,(2\varphi)$$

For the tapered region we have:

$$N_x^s = j\pi\,dz\,sin(2\varphi)\sum_{i=1}^{N}\frac{\beta_i}{k_{\rho i}}A_i(1+s_i)I_{3i}e^{jk_0z_icos\,\theta}$$

$$N_y^s = j\pi dz\sum_{i=1}^{N}\frac{\beta_i}{k_{\rho i}}A_i[(1-s_i)I_{1i} - (1+s_i)I_{3i}cos(2\varphi)]e^{jk_0z_icos\,\theta} \quad (12)$$

$$N_z^s = -2j\pi\,dz\,sin(\varphi)\sum_{i=1}^{N}A_iI_{5i}e^{jk_0z_icos\,\theta}$$

Where we have defined:

$$I_1 = \int_0^a J_0(k_\rho\rho)J_0(k_0\rho sin\,\theta)\rho d\rho$$

$$I_2 = \int_a^\infty K_0(\alpha_\rho\rho)J_0(k_0\rho sin\,\theta)\rho d\rho$$

$$I_3 = \int_0^a J_2(k_\rho\rho)J_2(k_0\rho sin\,\theta)\rho d\rho \quad (13)$$

$$I_4 = \int_a^\infty K_2(\alpha_\rho\rho)J_2(k_0\rho sin\,\theta)\rho d\rho$$

$$I_5 = \int_0^a J_1(k_\rho\rho)J_1(k_0\rho sin\,\theta)\rho d\rho$$

Above integrals can be evaluated analytically [19].

III. NUMERICAL RESULTS

In order to validate the analysis technique presented here, numerical results are compared with the data obtained from CST Microwave Studio using a full-wave integral equation method. To ensure that the dominant HE_{11} mode is the only propagating mode in the feeding waveguide, the following relationship must hold:

$$\frac{2a_0}{\lambda_0} = \frac{2.4049}{\pi\sqrt{\varepsilon_r - 1}} \quad (14)$$

As long as $a(z)$ remains smaller than a_0, only the fundamental surface wave mode remains above cutoff. In this paper, two types of taper profiles are investigated: the first one is a linear taper and the other is a sinusoidal profile with exponential decay which is defined by:

$$a(z) = 0.25a_0\left[3 + cos\left(\frac{n\pi z}{L}\right)\right]exp\left(-\alpha\frac{z}{L}\right) \quad (15)$$

in which "n" is an integer and L is the length of the tapered rod antenna. In this paper a lossless dielectric rod with a relative permittivity of $\varepsilon_r = 2$ (Teflon) and with a $10\lambda_0$ taper section with the starting radius of $0.32\lambda_0$ and the minimum radius of $0.16\lambda_0$at f=11 GHz was considered. For the sinusoidal profile, n=19, 55 and $\alpha = 0.25$ were assumed.

As shown in Fig. 4 and 5 for the linearly tapered antenna, very good agreement is observed between the proposed method and the commercial simulator. In this case the calculated and the simulated gains are 17.72dB and 17.8dB, respectively. The calculated HPBW is 23.2° while the simulated one is 22.8°. In this case the antenna is fed by a uniform dielectric rod.

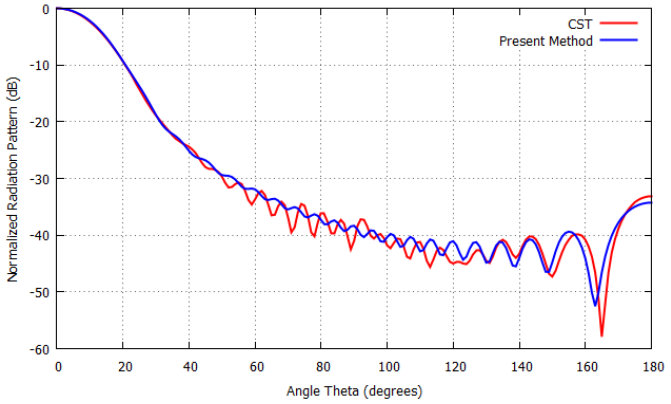

Fig. 4. H-plane radiation pattern for a $10\lambda_0$ long linear tapered rod with $\varepsilon_r = 2$, $a_0 = 0.32\lambda_0$ and $a_{min} = 0.16\lambda_0$ at 11GHz fed by a uniform dielectric waveguide.

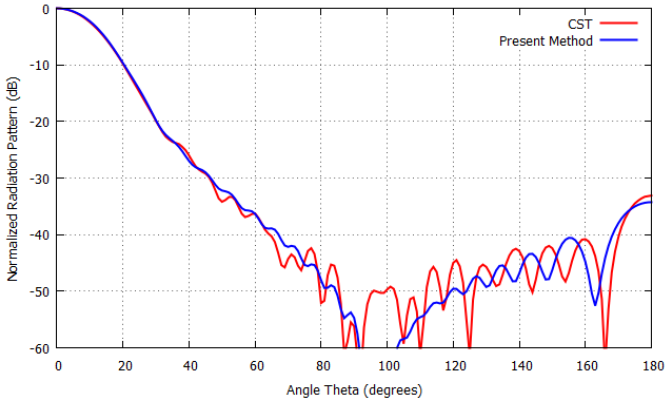

Fig. 5. E-plane radiation pattern for a $10\lambda_0$ long linear tapered rod with $\varepsilon_r = 2$, $a_0 = 0.32\lambda_0$ and $a_{min} = 0.16\lambda_0$ at 11GHz fed by a uniform dielectric waveguide.

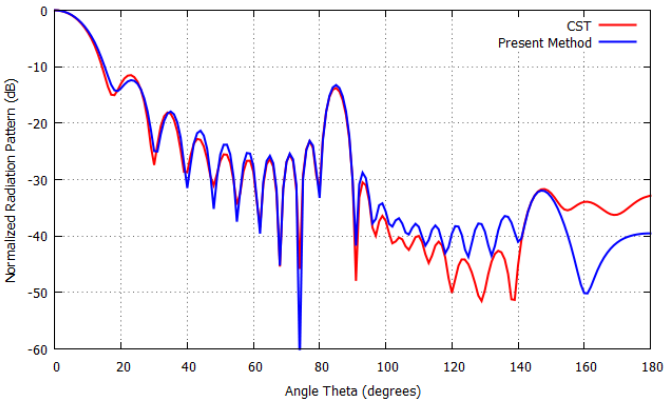

Fig. 6. H-plane radiation pattern for a $10\lambda_0$ long periodically tapered rod with n=19, $\varepsilon_r = 2$ and $a_0 = 0.32\lambda_0$ at 11GHz fed by a uniform dielectric waveguide.

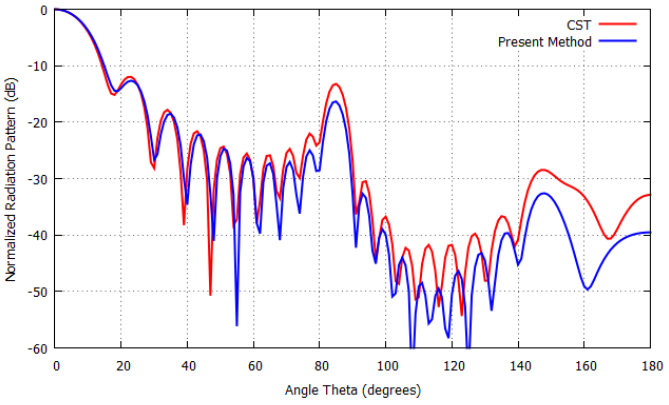

Fig. 7. E-plane radiation pattern for a $10\lambda_0$ long periodically tapered rod with n=19, $\varepsilon_r = 2$ and $a_0 = 0.32\lambda_0$ at 11GHz fed by a uniform dielectric waveguide.

For the decaying sinusoidal profile fed by a uniform dielectric rod, as shown in Fig. 6 and 7, again a very good agreement is observed between the proposed method and CST Microwave Studio. In this case the calculated gain is 18.46dBi and the simulated one is 18.5dBi. The calculated HPBW is 18.3° while the simulated one is around 17.7°. With increasing the number of periods 'n' the side lobe seen around $\theta = 85°$, moves towards the back side and with further increase of 'n' it reaches $\theta = 180°$. This side lobe is due to radiation from the leaky mode that is reflected from the end and travels backward along the rod. A higher gain can be achieved with increasing 'α' in (15) and the antenna length 'L'. Radiation patterns are plotted for $n = 55$ in Fig. 8 and 9. It can be seen that the unwanted side-lobe is eliminated. In this case the calculated gain is about 19.4dB and the simulated gain is 19.2dB.

The method presented in [14] does not take the feeding mechanism of the antenna into consideration but our method can be used with various excitation methods such as electric or magnetic dipoles or TE_{11} circular waveguide excitation. For these types of excitations, the method in [14] requires that the total power carried by the taper field to be a constant independent of z which is not true. Because for real excitation methods many modes of the dielectric waveguide can be excited including the radiation modes, therefore there will be some radiation loss that cannot be taken into account by the local mode theory. For a y-directed electric dipole placed at the origin and TE_{11} circular waveguide feed, radiation patterns are calculated and shown in Fig. 10 and 11. Note that (9) and (10) must now be replaced with appropriate expressions.

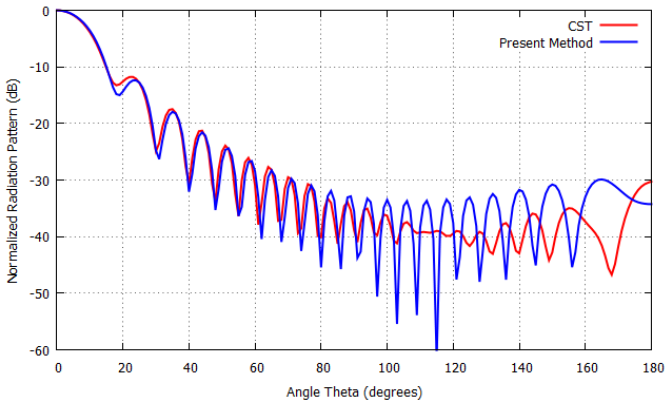

Fig. 8. H-plane radiation pattern for a $10\lambda_0$ long periodically tapered rod with n=55, $\varepsilon_r = 2$ and $a_0 = 0.32\lambda_0$ at 11GHz fed by a uniform dielectric waveguide.

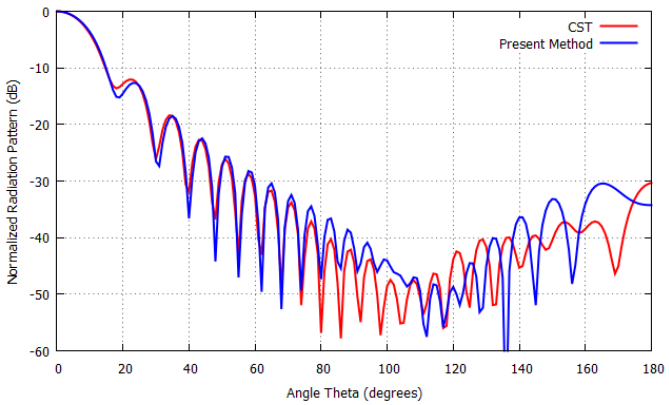

Fig. 9. E-plane radiation pattern for a $10\lambda_0$ long periodically tapered rod with n=55, $\varepsilon_r = 2$ and $a_0 = 0.32\lambda_0$ at 11GHz fed by a uniform dielectric waveguide.

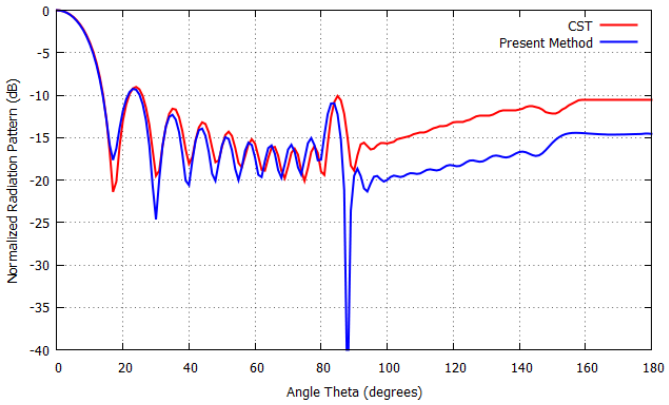

Fig. 10. H-plane radiation pattern for a $10\lambda_0$ long periodically tapered rod with n=19, $\varepsilon_r = 2$ and $a_0 = 0.32\lambda_0$ at 11GHz excited by a y-directed electric dipole.

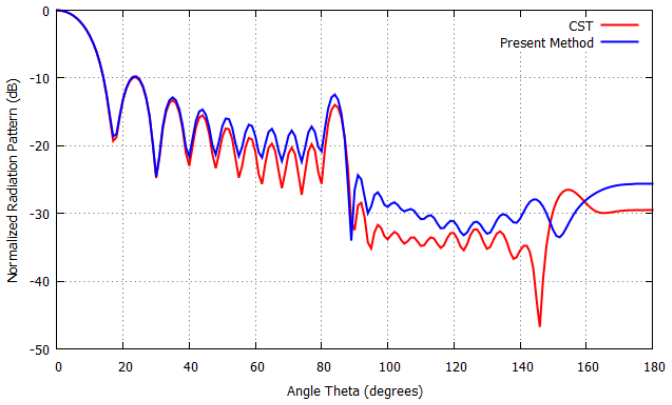

Fig. 11. H-plane radiation pattern for a $10\lambda_0$ long periodically tapered rod with n=19, $\varepsilon_r = 2$ and $a_0 = 0.32\lambda_0$ at 11GHz excited by a TE_{11} circular waveguide.

As shown in Fig. 10 and Fig. 11, there is a good agreement between the proposed method and the commercial EM simulator except for the back radiation which is mainly due to the radiation from the feed which was not included in our approach. This method can be used in any tapered dielectric antenna as long as its transverse fields can be approximated by the local mode theory, so the method is not restricted to circular rod antenna.

Evaluating a profile in Matlab at a single frequency took about 70 seconds on a laptop with a 64-bit 2.5 GHz dual core processor utilizing one core and 4 GB RAM, whereas CST Microwave Studio took at least about 15 minutes on both cores, depending upon the meshing density.

IV. CONCLUSION

The use of both equivalent volume current distributions with a local mode approximation for the fields in the tapered dielectric region provided a fairly accurate and computationally efficient method for computation of the radiation pattern for tapered dielectric antennas. Accurate results can be expected as long as the taper profile is gradual and the antenna cross-section varies slowly. This method can be used efficiently for the design and optimization of such antennas.

REFERENCES

[1] F. Schwering and A. A. Oliner, "Millimeter-wave Antennas", in *Antenna Handbook*, Y. T. Lo and S. W. Lee, Eds., Van Nostrand Reinhold, New York, 1988.

[2] H. Jacobs and M. M. Chrepta, "Electronic phase shifter for millimeter-wave semiconductor dielectric integrated circuits," *IEEE Trans. Microw. Theory Tech.,* vol. MTT-22, no. 4, pp. 411 –417, Apr. 1974.

[3] R. Baets and P. E. Lagasse, "Calculation of radiation loss in integrated-optic tapers and Y-junctions," *Appl. Opt.,* vol. 21, no. 11, pp. 1972 – 1978, Jun. 1982.

[4] F. J. Zucker and W. F. Croswell, "Surface-wave antennas," in *Antenna Engineering Handbook*, J. L. Volakis, Ed., 4th ed. New York: Mc-Graw-Hill, 2007, ch. 10.

[5] F. J. Zucker and R. C. Johnson. "Surface-wave antennas and surface-wave excited arrays," in *Antenna Engineering Handbook*, chapter 12. McGraw-Hill, New York, 3rd edition, 1993.

[6] F. Schwering, A. A. Oliner, Y. T. Lo, and S. W. Lee. "Millimeter-wave antennas," in *Antenna Handbook*, volume 3, chapter 17. Van Nostrand Reinhold, New York, 1993.

[7] C.-C. Chen, K. R. Rao, and R. Lee. "A new ultrawide-bandwidth dielectric-rod antenna for ground-penetrating radar appli-cations," *IEEE Trans. Antennas Propag.*, 51(3):371–377, March 2003.

[8] T. Ando, J. Yamauchi, and H. Nakano. "Numerical analysis of a dielectric rod antenna - demonstration of the discontinuity-radiation concept," *IEEE Trans. Antennas Propag.*, 51(8):2007–2013, Aug. 2003.

[9] T. Ando, I. Ohba, S. Numata, J. Yamauchi, and H. Nakano. "Linearly and curvilinearly tapered cylindrical dielectric-rod antennas," *IEEE Trans. Antennas Propag.*, 53(9):2827–2833, Sept. 2005.

[10] A. Kishk and L. Shafai. "Radiation characteristics of the short dielectric rod antenna: A numerical solution," *IEEE Trans. Antennas Propag.*, 35(2):139–146, Feb 1987.

[11] J. Blakey. "A scattering theory approach to the prediction of dielectric rod antenna radiation patterns: The TM01 mode," *IEEE Trans. Antennas Propag.*, 23(4):577–579, Jul 1975.

[12] J. Ma Gil, J. Monge, J. Rubio, and J. Zapata. "A cad-oriented method to analyze and design radiating structures based on bodies of revolution by using finite elements and generalized scattering matrix," *IEEE Trans. Antennas Propag.*, 54(3):899–907, March 2006.

[13] G. M. Whitman, C. Pinthong, A. A. Triolo, and F. K. Schwering. "An approximate but accurate analysis of the dielectric wedge antenna fed by a slab waveguide using the local mode theory and schelkunoff equivalence principle," *IEEE Trans. Antennas Propag.*, 54(4):1111–1121, April 2006.

[14] E. Niver. "Tapered dielectric rod antenna," in *Complex Computing Networks*. Springer, 2006.

[15] G. M. Whitman, F. Schwering, W.-Y. Chen, A. Triolo, and J. Junnapart, "The Integrated dielectric slab waveguide-wedge antenna," in *Directions for the Next Generation of MMIC devices and Systems,* N. K. Das and H. Bertoni, Eds. New York: Plenum Press, 1997, pp. 181–195.

[16] F. Schwering, G. M. Whitman, A. Triolo, and W.-Y. Chen, "The dielectric wedge antenna fed by a slab waveguide using local mode theory and equivalent current distributions: TE case," presented at the Int. IEEE AP-S Symp. and URSI Meeting, Newport Beach, CA, Jun. 19–23, 1995.

[17] K. Okamoto. *Fundamentals of Optical Waveguides*. Academic Press, 2000.

[18] R. F. Harrington. *Field Computation by Moment Methods*. IEEE Press, 2000.

[19] I. S. Gradshteyn and I. M. Ryzhik, *Table of Integrals, Series, and Products*, 7th edition, Elsevier Inc., London, 2007.